A novel damage assessment method in Peridynamic simulations

Hamarat, Mehmet; Kaewunruen, Sakdirat

DOI:
10.1016/j.apm.2023.06.038

Document Version
Publisher's PDF, also known as Version of record

Citation for published version (Harvard):
Hamarat, M & Kaewunruen, S 2023, 'A novel damage assessment method in Peridynamic simulations', *Applied Mathematical Modelling*, vol. 123, pp. 274-294. https://doi.org/10.1016/j.apm.2023.06.038

Applied Mathematical Modelling 123 (2023) 274–294

Contents lists available at ScienceDirect

Applied Mathematical Modelling

journal homepage: www.elsevier.com/locate/apm

A novel damage assessment method in Peridynamic simulations

Mehmet Hamarat[a,b], Sakdirat Kaewunruen[a,*]

[a] Birmingham Centre for Railway Research and Education, School of Engineering, The University of Birmingham, B15 2TT, United Kingdom
[b] School of Engineering, Bogazici University, 34342, Turkiye

ARTICLE INFO

Article history:
Received 7 April 2023
Revised 15 June 2023
Accepted 30 June 2023
Available online 6 July 2023

Keywords:
Peridynamics
Crack
Damage assessment
Crack propagation
Crack initiation

ABSTRACT

This paper proposes a novel approach to evaluate the damage in Peridynamic simulations to identify the crack initiation and propagation, based on the physical meaning of the bond network. The most commonly used criterion to assess the damage in Peridynamic simulations is the nodal damage value, a ratio of the broken bonds to number of unbroken bonds for each point. There is no consensus on the magnitude of nodal damage value within the literature. In most cases, the assessment is conducted visually via damage contours. Rarely, researchers calculate nodal damage value by counting the bonds that pass through a crack plane and must be broken to initiate a crack. Despite being widely-used, the application of nodal damage value is questionable since it neglects the likelihood of broken bonds that are irrelevant to a crack. In other words, the applied value of the nodal damage value might not give the information about the crack whether it emerges or not. This paper shows the influence of the nodal damage value on damage assessments and compares the proposed method with the nodal damage value in different scenarios. The results exhibit that the proposed method is robust, effective, and more importantly provides a single outcome for Peridynamic simulations.

1. Introduction

In the last two decades, numerical methods have featured prominently to solve many problems ranging from nano scale to macro scale in engineering and science. Within the literature, there are many methods having unique properties and limitations associated with the definition of the problem. Probably, the most common and flexible method is the renowned Finite Element Method (FEM), which utilizes classical continuum theory (CCT). Despite its superiority, the mathematical framework of CCT has flaws while solving certain problems that present large deformations and discontinuities which cannot be defined by partial derivatives [1]. Particularly, it is a great challenge in fracture mechanics with regard to crack discontinuity and crack tip singularity that are of the subject. Many remedies such as special elements, advanced numerical algorithms or specific evaluation techniques are proposed to get around such problems originating from CCT [2,3]. However,

* Corresponding author.
E-mail address: S.Kaewunruen@bham.ac.uk (S. Kaewunruen).

https://doi.org/10.1016/j.apm.2023.06.038

the applications of those solutions are custom-tailored and require expert knowledge, thus, reducing the usefulness of FEM in most cases.

To overcome the burdens of FEM, a new formulation of a continuum model was introduced at the beginning of the current millennia, so-called 'Peridynamics' (PD) that means 'Near Forces' in Greek [4]. Peridynamic theory is fundamentally devoid of partial differential equations and inherently effective to solve problems including large displacements and discontinuities. In Peridynamic theory, the motion of equation is determined by the forces acting between the points of interest and their neighbours. Those forces are referred as bond forces and the distance between two neighbours is represented by a virtual bond. In other words, in PD, a motion of a point in a body can be described by the motions of all other points within a certain distance, which produce forces on the point of interest. PD is able to deal with the discontinuities within the body trivially by employing integration of the forces between neighbouring points. The original or early version of PD is called "Bond-based PD". Nevertheless, it captures Poisson's ratios of 0.33 in 2D (plane stress) and 0.25 in 3D (the same for plane strain in two-dimension) automatically, which ensures the validity of theory only for elastic materials with certain Poisson's ratio. In 2007, the theory was reformulated and a more generalized formulation of PD was developed, referred to as "State-based PD" which is more flexible in terms of Poisson's ratio in comparison to "Bond-based PD"[5]. In details, the state-based PD is established on two different formulations such as ordinary and non-ordinary [5]. By definition, the ordinary PD considers that the forces acting between two neighbour nodes are colinear whereas non-ordinary formulation concerns arbitrary interaction between those nodes. The basis of non-ordinary state-based PD formulation is to reflect the material behaviour in a similar way in classical continuum theory such that the interactions between nodes are represented with conventional strain and stress tensors enabling the use of the general constitutive models [6]. It is worth mentioning that ordinary state-based theory requires new constitutive equations for each material. Despite sounding attractive, the main challenge in the application of non-ordinary state-based PD is the stability problem as demonstrated in [7]. In recent years, several studies proposed more stable material models for non-ordinary state-based PD [8–10]. Yet, those non-ordinary material models have some drawbacks such as being more computationally expensive than the general non-ordinary state-based models. Consequently, there is no superiority amongst the versions of PD. All three versions of PD are still in use and development.

The potential of PD has been proved in numerous studies. PD has been applied to many problems including but not limited to stationary cracks [11,12], thermal cracks [13,14], dynamic cracks [15,16], fatigue cracks [17–20]. PD also provides considerable flexibility in terms of material models. Various material models (i.e. elastic, plastic, viscoelastic, hyperplastic, composites, polycrystalline) are successfully developed and implemented in PD [4,21–24]. Furthermore, PD could be coupled with classical continuum methods such as FEM, to exploit the advantage of both methods [25,26]. Despite its power to eliminate the limitations that are encountered in classical continuum theory, there are also some challenges to be addressed in PD. For instance, the influence of discretization parameters [8,10], surface effects [27,28] and being computationally expensive [29] are some of the challenges in PD theory.

In PD, a common approach to assess the failure is to define nodal damage value(NDV) that will represent the crack. The challenge, here, is to determine the nodal damage value itself. Even though the assessments are mostly qualitative and the approach reflects the result at some degree, the nature of the approach is questionable. For instance, crack profile, length and propagation speed can be manipulated to achieve desired outcomes by adjusting the nodal damage value. Likewise, it is a significant question in fatigue modelling [17], where it was said that phase transition from crack initiation to propagation was related to the nodal damage value but the description of how to determine nodal damage value was not given. In order to avoid the subjective concept of nodal damage value, there have been manual attempts to determine the nodal damage value in a more objective way [19,20,30]. For that purpose, basically, a line or plane is drawn as a crack path and then the number of bonds to be broken is manually counted to calculate the nodal damage value. However, this method ignores the possibility of broken bonds that do not intersect with the crack plane. It is noteworthy that damage criteria could also be a modification of nodal damage value in some cases [31], which is still subjected to same question. Apart from the nodal damage value, critical energy release criteria, a quantitative approach, is offered in [32]. Yet, the study is limited to a simple geometry with a stationary crack due to the total energy approach and the preferred definition of critical energy release rate. Furthermore, critical energy release methods cannot be applicable for fatigue crack growth [33]. Briefly, there is a necessity to define the failure or to trace the crack propagation more accurately. Recently, a new method has been proposed to solve the problem [34]. However, the proposed solution neglected the non-local nature of PD. This paper presents, based on the physical meaning of the crack and non-local nature of PD, a novel approach that states "a crack will occur between two closest neighbour points that lose all direct and first-degree indirect contact". It is the first time that this approach is established to define the failure in PD simulations. It is believed that the method can be utilized with any Peridynamic model. Throughout this paper, the state-based Peridynamics is preferred for convenience in our simulations.

2. Methodology

2.1. Theory of Peridynamics

In this section, Peridynamics (PD) theory will be briefly explained. More detailed explanation of the theory could be found in [1,4–6]. The basis of the PD theory is similar to conservation of the momentum. For any point in a body that

occupies a reference configuration in space, the force per unit reference volume can be defined by

$$\mathbf{L}(\mathbf{x},\mathbf{t}) = \int_{H_x} \mathbf{f}\left(\mathbf{u}\left(\mathbf{x}',t\right)-\mathbf{u}(\mathbf{x},\mathrm{t}),\mathbf{x}'-\mathbf{x}\right).dV_{x'} \tag{1}$$

where $\mathbf{f}$, $\mathbf{u}(\mathbf{x}', t) - \mathbf{u}(\mathbf{x}, t)$, $\mathbf{x}' - \mathbf{x}$, $V_{x'}$ are a pairwise vector-valued force function between the points and their neighbours, displacements of the points and their neighbours, initial distance between each point-neighbour pairs and volumes of each neighbour point, respectively. H_x, so-called horizon, is the range for identifying neighbours. Beyond the horizon, $\mathbf{f} = 0$. PD equation of motion is given by

$$\rho(x).\ddot{\mathbf{u}}(\mathbf{x},t) = \mathbf{L}(\mathbf{x},t) + \mathbf{b}(\mathbf{x},t) \tag{2}$$

where $\rho(x)$ is the density of point x and $\mathbf{b}(\mathbf{x}, t)$ is the external force vector per unit reference volume, acting on the point. The bond, which will be represented by $\boldsymbol{\xi}$ later, is a PD jargon for $\mathbf{x}' - \mathbf{x}$. Similarly, $\boldsymbol{\eta}$ will show the relative displacement of the bond,$\mathbf{u}(\mathbf{x}', t) - \mathbf{u}(\mathbf{x}, t)$. For a linear elastic isotropic solid, the $\mathbf{f}$ is expressed as

$$\mathbf{f}\left(\mathbf{x},\mathbf{x}',t\right) = Cs.\frac{\boldsymbol{\eta}+\boldsymbol{\xi}}{\left|\boldsymbol{\eta}+\boldsymbol{\xi}\right|}\ C = \frac{12E}{\pi\delta} \text{ and } s = \frac{|\boldsymbol{\eta}|}{|\boldsymbol{\xi}|} \tag{3}$$

where C is a material constant, E is the modulus of elasticity, δ is the radius of horizon and s is the PD bond stretch. As seen from Eq. (3), only one parameter of Lame parameters (E,ν) exists in the pairwise force function. Since Poisson's ratio cannot be selected freely, this version of PD theory, "Bond-based Peridynamic", is valid for the Poisson's ratio of 0.33 in two-dimension (plane stress) and 0.25 in three-dimension (the same for plane strain in two-dimension) [29]. Due to limitations of bond-based PD, the motion of equation was upgraded as follows,

$$\rho(\mathbf{x}).\ddot{\mathbf{u}}(\mathbf{x},t) = \int_{H_x} \left\{\underline{\boldsymbol{T}}(\mathbf{x},t)\langle\mathbf{x}'-\mathbf{x}\rangle - \underline{\boldsymbol{T}'}\left(\mathbf{x}',t\right)\langle\mathbf{x}-\mathbf{x}'\rangle\right\}.dV_{x'} + \mathbf{b}(\mathbf{x},t) \tag{4}$$

where $\underline{\mathbf{T}}(\mathbf{x}, t)\langle\mathbf{x}' - \mathbf{x}\rangle$ is called force state. For the convenience, the notation of states will be simplified such that the force state will given as $\underline{\mathbf{T}}$ instead of $\underline{\mathbf{T}}(\mathbf{x}, t)\langle\mathbf{x}' - \mathbf{x}\rangle$. The term "state" is a basically an array that holds the information about PD bonds. For instance, deformation($\underline{\mathbf{Y}}$) and force states ($\underline{\mathbf{T}}$) of the point x_i can be written such that,

$$\underline{\mathbf{Y}}\begin{Bmatrix} y_1 - y_i \\ \cdots \\ y_n - y_i \end{Bmatrix} = \underline{\mathbf{T}}\left(\underline{\mathbf{Y}}_{x_i}\right) = \begin{Bmatrix} t_{1,i} \\ \cdots \\ t_{n,i} \end{Bmatrix} \tag{5}$$

where the n and t indicate the number of neighbours of the point x_i and the force between two neighbours. It is noteworthy that states are mathematically defined special tensors-like object [5] having its own rules. Hence, each state might have different properties. For instance, force state is dependant on deformation state whereas deformation state is independent as can be seen in Eq. (5).

The correlation between force and deformation states depends on the state-based material models. As mentioned in the introduction, there are many material models in the literature. Here, a brief explanation could be provided for the difference between ordinary and non-ordinary state-based PD materials, which is related to how to define the relation between force state and deformation state. Assume a state called "deformed direction vector state ", $\underline{\mathbf{M}}$ that is defined by $\underline{\mathbf{M}}(\underline{\mathbf{Y}}) = dir\,\underline{\mathbf{Y}}$ and the relation between $\underline{\mathbf{T}}$ and $\underline{\mathbf{M}}$ is established in Eq. (6).

$$\underline{\mathbf{T}} = \underline{t}.\underline{\mathbf{M}} \tag{6}$$

where $\underline{t}$ *is* a scalar force state field. If a material has a scalar state for any deformation, then material is an ordinary material and the PD theory using this material is called "Ordinary State-Based PD". Otherwise, the material is non-ordinary and must satisfy the conservation of angular momentum, which is defined in Eq. (7).

$$\int_{H_x} \{\underline{\mathbf{Y}} \times \underline{\mathbf{T}}\}.dV_{x'} = 0 \tag{7}$$

As aforementioned, non-ordinary materials are expected to behave like classical continuum materials and can be related to stress and strain terms. This relation is provided by

$$\underline{\mathbf{T}} = \underline{w}\ \boldsymbol{P}\ \boldsymbol{K}^{-1} \text{ and } \boldsymbol{K} = \int_{H_x} \underline{w}(\underline{\mathbf{X}} \otimes \underline{\mathbf{X}}).dV_{x'} \tag{8}$$

where $\boldsymbol{P}$ is Piola stress tensor, $\boldsymbol{K}$ is the shape tensor, $\underline{\mathbf{X}}$ is the reference position state and $\underline{w}$ is the influence function state that weighs the contribution of each bond. It should be emphasized that the influence function can be utilized to break so-called bonds between the point x_i and its neighbour x_j; and to define the damage for the point x_i. For instance, it can be set to zero if the stretch of a bond exceeds certain value. Then, the ratio between damaged bonds and undamaged bonds gives a damage value for the relevant point in Eq. (9).

$$w\left(x_{ij}\right) = \begin{cases} 1\ if\ s_{ij} < s_c \\ 0\ if\ s_{ij} > s_c \end{cases} \text{ And } \phi(x_i) = 1 - \frac{\int_{H_x} w\left(x_{ij}\right).dV_{x'}}{\int_{H_x} dV_{x'}} \tag{9}$$

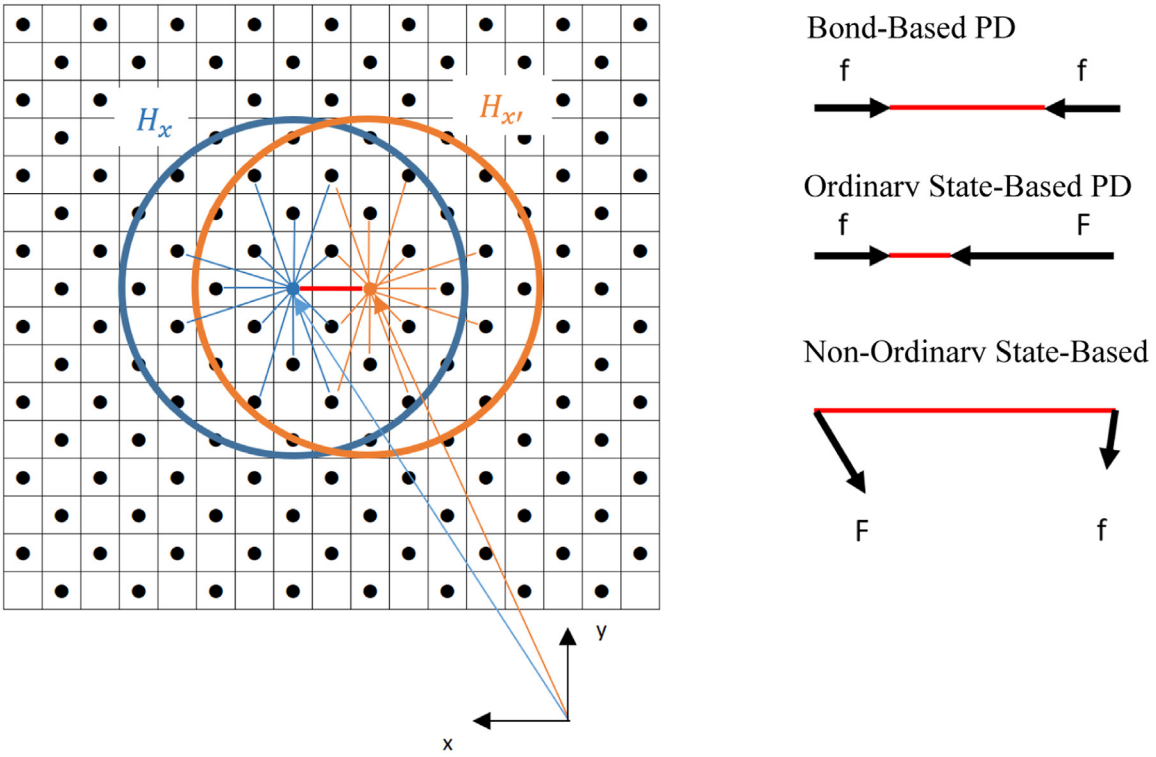

Fig. 1. An illustration of PD theory.

where $w(x_{ij})$,s_{ij}, s_c are the influence function, the stretch between the point x and its neighbour x' and critical stretch value to break the bonds. Likewise, $\phi(x_i)$ is the nodal damage value of the point x. Here, it is crucial to emphasize that the expressions in Eq. (9) could be the most common method to introduce damage in PD simulations. In Eq. (9), $w(x_{ij})$ is the simplest condition called as "Critical Stretch Criteria"; can be labelled as "bond-breaking criteria" and be set different with reference to the material model. On the other hand, $\phi(x_i)$ in Eq. (9) is a way of assessing the damage and can be applicable to any material model. It is a qualitative assessment and the most common method, which will be called as "nodal damage value" throughout this paper. Indeed, it can be the only method since the quantitative method offered in [32] is limited to certain type of geometry and valid for stationary crack due to definition of critical released energy. The critical released energy was defined in [32] as,

$$w_s = \frac{1}{2} G_0 B \Delta x \tag{10}$$

where w_s is the critical released energy of the crack surface, G_0 is the Griffith's critical released energy of the material, B is the thickness of the specimen and Δx is the unit crack propagation. Since the crack propagation surfaces cannot be defined in many applications and Griffith's approach is limited to certain scenarios, the proposed methodology in [32] cannot be used as a general criterion.

2.2. The method of "Close neighbour and crack on mid-plane"

An illustration of Peridynamics (PD) theory in two dimension is given in Fig. 1. The motion of the point x, blue dot is influenced by bond forces between the point and its neighbours. It should be emphasized that not all the bonds are illustrated in the Fig. 1 to present a clear picture. One of the neighbours is point x', orange dot, motion of which is also defined by its own neighbours. The bond force between two points could be in three different configurations, which represent three versions of PD theory (as shown in Fig. 1).

As illustrated in Fig. 1, PD theory considers the physics of material points via bonds somehow rather than mathematics. In other words, the concept of bond represents something physical. Therefore, based on this physical meaning, the damage criteria could be established in a similar way.

Due to its non-local property of PD, the points within the body influence each other "directly" when they are neighbours and "indirectly" when they have common neighbours. The indirect interaction between points that have common neighbours is called first-degree indirect contact. It is crucial to remind that PD geometry is a network of bonds in which points can influence each other via bond network. Nonetheless, those interactions are weak in comparison to direct and first-degree

indirect contact. Based on this definition, the proposal for damage criteria can be set as

$$R_x = \left\{x' \in \beta : \ 0 < \left|x' - x\right| < \delta \ \wedge \ w\left(\left|x' - x\right|\right) \neq 0, \ x \in \beta\right\} \tag{11}$$

$$\phi(x_i), \phi\left(x_j\right) = \begin{cases} 0 & if \ \left|x_j - x_i\right| \langle c \ \wedge \ R_{x_i} \cap R_{x_j} \ \neq 0 \ or \ if \ \left|x_j - x_i\right| \rangle c \\ 1 & if \ \left|x_j - x_i\right| < c \ \wedge \ R_{x_i} \cap R_{x_j} = 0 \ \wedge \ w\left(\left|\xi_{ij}\right|\right) = 0 \end{cases} \tag{12}$$

where R_x is a set of neighbour points of a point within the discretized body domain β; x_i and x_j are any two neighbour points in the body and c is the constant identifying the closest neighbours. The constant (c) is selected as $\Delta x\sqrt{2}$ to determine closest neighbours of the point of interest in a body that has a uniformly distributed mesh structure. Here, Δx means the initial distance between two adjacent nodes, where the horizon constant is $3\Delta x$. It is noteworthy that as aforementioned, the novel method proposes "a crack will occur between two nodes only if those nodes are in the closest vicinity". That is why the nodes having $|x_j - x_i| > c$ cannot produce a crack.

The equations of Eqs. (11) and (12) mean that damage will occur between those two close neighbours if they lose their direct and indirect contact. Here, it should be noted that the general notation, ϕ, is used to define a crack. However, this notation has a slight different meaning in the proposed method such that a crack occurs between two damaged points ($\phi = 1$) and those points might bear loads in other directions.

The basis of the assumption of two-close neighbour is that there will be always closest neighbours surrounding a crack (i.e. x" and x') even if the first broken bonds belongs to a point x and its far neighbour x'. The application of proposed method is computationally demanding due to the number of subsets of $\mathcal{R}_x$. Therefore, the proposed method is simplified further. Assume there exist a plane, $\mathcal{P}$, between the point x and its closest neighbour point x' and there is a function that defines the relation between bonds and broken bonds of those two points that pass through this plane Eqs. (13), ((14)).

$$\mathrm{Z}(x) = \int_{\mathcal{P}} \left(1 - w\left(\left|\xi\right|\right)\right) dA \tag{13}$$

$$\phi(x), \phi\left(x'\right) = \{ \begin{matrix} 1 & if \ \mathrm{Z}(x) = 0 \ \wedge \ \mathrm{Z}\left(x'\right) = 0 \\ 0 & else \end{matrix} \tag{14}$$

where P,A are a plane and areas of the bonds on that plane. To facilitate the problem, the formula of the plane $\mathcal{P}$ can be defined as,

$$\boldsymbol{\xi} \ . \ (\ \boldsymbol{p} - \boldsymbol{p}_0) = 0 \tag{15}$$

where $\boldsymbol{p}$, $\boldsymbol{p}_0$ are two points on the plane. A suitable selection of $\boldsymbol{p_o}$ is the mid-point of the points x and x'. Then, for any point $\boldsymbol{p}$, Eq. (15) defines a plane between the points x and x', which is perpendicular to $\boldsymbol{\xi}$. Hence, the proposed method is called as "Crack on Mid-Plane". It is worth mentioning that the crack planes will be rotated and moved with respect to positions of the bonds.

To increase the efficiency, one more condition in Eq. (16) can be introduced.

$$\mathcal{P} \in \mathcal{R} \ \boldsymbol{if} \ w\left(\left|\xi\right|\right) = 0 \tag{16}$$

In the numerical procedure, the above condition produce the mid-point plane when the relevant bond is broken instead of creating planes for each closest neighbours at the beginning of the simulation.

The computational routine for the method of "crack on mid-plane" is depicted in Fig. 2. The procedure starts by creating planes between point and its neighbours if the bond between those points are broken. At this point, planes have no geometrical meaning yet. They are composed of a group of arrays providing relevant information such as point ID, neighbour ID, the bond identification index, plane identification index and so on. Having created all the planes at the locations of broken bonds, another function is called for every plane of the point x to create geometrical planes for the point x. Then, the same function is called to check all the bonds belonging to the point x whether they intersect the plane or not. Simultaneously, the function also checks whether the intersecting bonds are broken or not. In the final step, the procedure calls another function that checks the condition in Eq. (14). If the condition is satisfied, a crack develops at that location.

3. Results and discussions

In this section, the proposed method is investigated by using four examples. The method is implemented in the open-source code of Peridynamics (PD), called "Peridigm" [35]. All other elements of a peridynamic simulation ranging from material models to surface effects treatment are used from the library of Peridigm.

Due to computational costs, the simulations are conducted on a High Performance Computing (HPC) system, which also limits the number of cases. The cost of the proposed method is approximately 2x (in Case 1), 1.7x (in Case 2), 1.2x (in Case 3) and 1.4x (in Case 4) times higher than normal run that can be used to assess damage by nodal damage value. The word "approximately" is used since the performance of the system depends on several parameters that cannot be controlled by the user of HPC system.

Algorithm. The routine for the method of "Crack on Mid-plane"

```
procedure Crack on Mid-plane
    % Create planes when a bond is broken
    for each node i do
        for each neighbour j do
            if bond(i,j) = = 1
            create plane
            end if
        end for

        %check whether bonds intersects the planes
        if plane exists on node i
            for each plane do
                for each neighbour j do
                function >> compute plane and bond intersection
                end for
            end for
        end if
    end for

    %check planes whether a crack occurs
    for each plane do
        function >> check crack propagation
    end for

function compute plane and bond intersection
    create vectors
    calculate intersection
    calculate angle
    if intersection = = true and angle <pi/2
        register bond(i,j)
        if bond(i,j) = =1
            register broken_bond(i,j)
        end if
    end if
end function

function check crack propagation
    if all bonds on the plane are broken
        register crack propagation
    end if
end function

end procedure
```

Fig. 2. The procedure for the proposed method.

3.1. Case 1 – fatigue crack propagation in a CT specimen

A simulation of a fatigue crack is simulated with Peridynamics (PD) theory. There are two models for fatigue cracking in the literature such as stretch-based [17] and energy-based approaches [19]. Both methods assign a certain value that represents total life, λ, to all bonds. In every cycle, the bonds gradually lose their life with respect to the magnitude of the stretch that they are subjected to or the magnitude of energy release from a bond due to bond deformation. The former is known as stretch-based fatigue model and the latter as energy-based fatigue model. Despite sounding similar, it is mentioned in [22] that the former is more suitable for elastic materials and the latter for plastic and composite materials.

A fatigue crack is simulated to show the effect of nodal damage value and the advantage of proposed method. The stretch-based fatigue model is preferred in this paper. The stretch-based method assumes in Eq. (17) that a bond has a finite life.

$$\lambda(0) = 1 \tag{17}$$

The life of the bond decrease when it is exposed to cyclic loadings and the function of degradation is given as

$$\frac{d\lambda}{dN} = -A\varepsilon^{m} \tag{18}$$

where A, m are material constants and ε, N represents stretch value and cycle, respectively. The material constants are extracted from experimental data by following the instructions in [17]. A bond will fail when it satisfies the condition in Eq. (19).

$$\lambda(0) - \int d\lambda = 0 \tag{19}$$

The damage will occur after sufficient number of failures of the bonds. In other words, the damage will be observed when the average damage of the node (the nodal damage value) reaches certain value as shown in Eq. (9). As aforementioned, the question is how to determine the nodal damage value to estimate the correlation between crack propagation and cycle.

To show the effectiveness of the proposed method, an experiment with a compact-tension(CT) specimen [36] is repeated in PD environment. The test material is 900A grade rail steel having the modulus of elasticity of 207 GPa and Poisson's ratio of 0.295. The dimensions of specimen are 50 × 48 × 10 mm (w x h x d). The positions of loading and initial crack complies with the standard [37]. The applied load is 14 kN with R ratio of 0.2. The geometry is discretized with 1 mm mesh and PD parameter horizon is selected as 3 mm ($3\Delta x$) with reference to recommendation in [1]. The PD model of the geometry is presented in Fig. 3a.

In Fig. 3b, the crack propagation that is estimated by proposed method is compared with experimental data from [36]. Apparently, the PD model with proposed method mimics the experiment with a negligible error. Particularly, the crack propagation curve of the model fits the experiment comprehensively. Nevertheless, one can realize that data points of the model indicating crack propagation speed in Fig. 3c slightly disagree with the experiment for lower stress intensity factors. The discrepancy between experiment and the model is related to the discretization of the geometry in PD, which is relatively large. Due to rough discretization, the model reaches the stable crack propagation stage later than the experiment. That difference is also perceptible in Fig. 3b. The density of the model data points is less than the experiment below 60,000 cycles in the figure, indicating that the less measurement points are available for the model. In other words, there is a data loss due to the lower resolution of the measurements which is directly related to discretization size. It is expected that fine meshes will increase conformity between experiment and model. Nevertheless, the correlation between fine meshes and computational cost is exponential in fatigue simulations as well as PD simulations.

In Fig. 3d, the proposed method is compared to four different nodal damage values in terms of crack length versus cycle. What stands out in the figure is that the nodal damage value influences the crack propagation, significantly. Regarding the proposed method as a reference, the deviations from the reference is related to the required number of broken bonds for each damage values. The higher the nodal damage value is, the higher the number of bonds is to be broken. Fig. 3d points out that the nodal damage value of 0.4 is the closest one to the proposed method. This value is slightly higher than the value in [20], which was 0.385. In [20], the possibility of a broken bonds in the opposite direction in comparison to direction of the most broken bonds was ignored.

Further explanations for certain behaviours in Fig. 3c must be provided for clarification. First, crack propagation speed, the gradient of the curves, changes suddenly for all damage values in the early stage of the crack propagation. This behaviour resulted from non-locality of PD that causes well-known surface effects [38]. Briefly, the points close to crack surfaces or domain boundaries in a distance less than the horizon will have lower number of bonds since they will have less neighbours in comparison to points within the body. Several remedies could be found within the literature [27,28,38,39]). Even though PD models are corrected with those solutions to some extent, most of the studies using nodal damage value as failure criteria seem to neglect surface effects in the calculation. Nevertheless, those remedies should also be applied to the nodal damage values. The nodes close to crack surface will have less bonds and therefore, damage criteria will be met earlier owing to definition of the nodal damage value. The second explanation is for the strange behaviour of crack propagation curve when nodal damage value of 0.45 is applied. When the selected nodal damage value is considerably high, the crack propagation must be high to break sufficient number of bonds to meet the criteria. Consequently, the crack propagates extremely slowly. When crack becomes unstable, crack speed increase rapidly. It is obvious in Fig. 3d that all the nodal

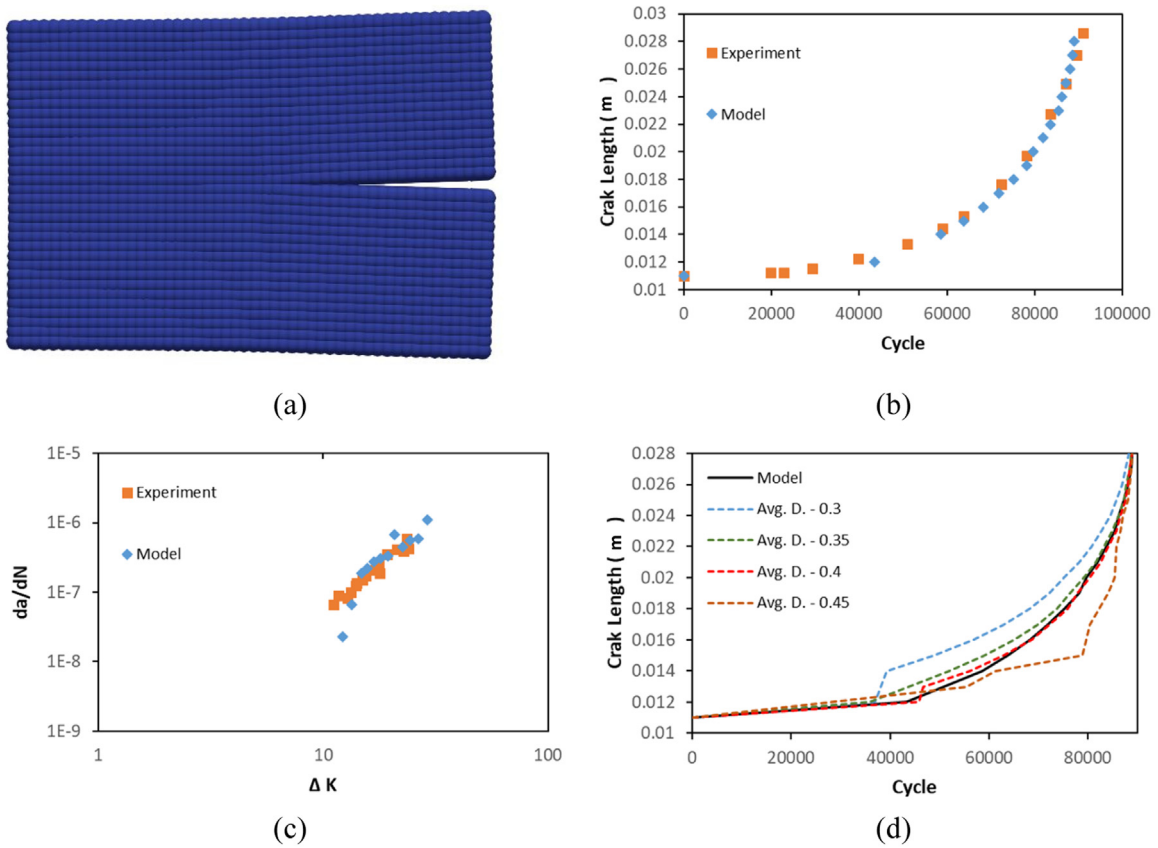

Fig. 3. (a) The geometry of PD fatigue model; (b) A comparison between experiment and model in terms of crack length and cycles; (c) A comparison between experiment and model in terms of crack propagation speed and stress intensity factor (note: da/dN is the fatigue crack growth rate, and ΔK is the stress intensity factor); (d) A comparison between different nodal damage value and proposed method.

damage values and proposed method converge at some point, when close to failure. Even though it looks strange at first, this behaviour is completely normal since the failure of the specimen is a physical phenomenon that take place in a certain time frame. The nodal damage value is a criterion to interpret the outcome.

Zoomed-in visuals of crack tip of the PD geometry for various nodal damage value and proposed method is presented in Fig. 4 for two different time steps. In Fig. 4a-e, the results are given for the time step when the proposed method captures crack propagation first time. It is clear in the figure that different nodal damage values produce different crack propagation speeds, associated with red points. Particularly, higher damage values cannot capture fatigue propagation at lower cycles. This outcome is also perceptible in Fig. 4a'-e', in which the crack length is provided after 59k cycles.

3.2. Case 2 – crack propagation due to impact

A recent study [40], in which several nodal damage values were also compared in terms of crack propagation speed, is partially repeated to show the advantage of proposed method. It is noteworthy that the word "partially" is used since a small part of the referred study is considered and State-based Peridynamics (SBPD) are used instead of Bond-based Peridynamics (BBPD) in the current study. In fact, BBPD had also been tried but it was not possible to repeat the study exactly due to nature of PD which seems to produce infinite number of results under impact loadings with respect to slight differences in PD parameters such as contact parameters, the position of the impact and so on, which are not mentioned in the reference. Since the major behaviours in [40] are captured in the current model, SBPD is preferred for convenience owing to aforementioned advantages of SBPD.

Two parts of the referred study is repeated. In the first part, an iron ball hits a thick layer soda-lime glass plate with different impact velocities ranging from 50 to 250 m/s, which is used to validate the model. The modulus of elasticity and fracture energy of the glass plate are given as 72 GPa and 0.007 kJ/m^2 and that of the steel ball are 200 GPA and 10 kJ/m^2,respectively. In the second part, the study investigates the fracture behaviour of a bullet hitting a cylindrical glass plate with a velocity of 100 m/s. The radius and thickness of the plate is 37 mm and 2.5 mm, respectively. The elastic modulus and fracture energy of the glass in that case are 94.5 GPa and 4.3 J/m^2. The material of the bullet is copper

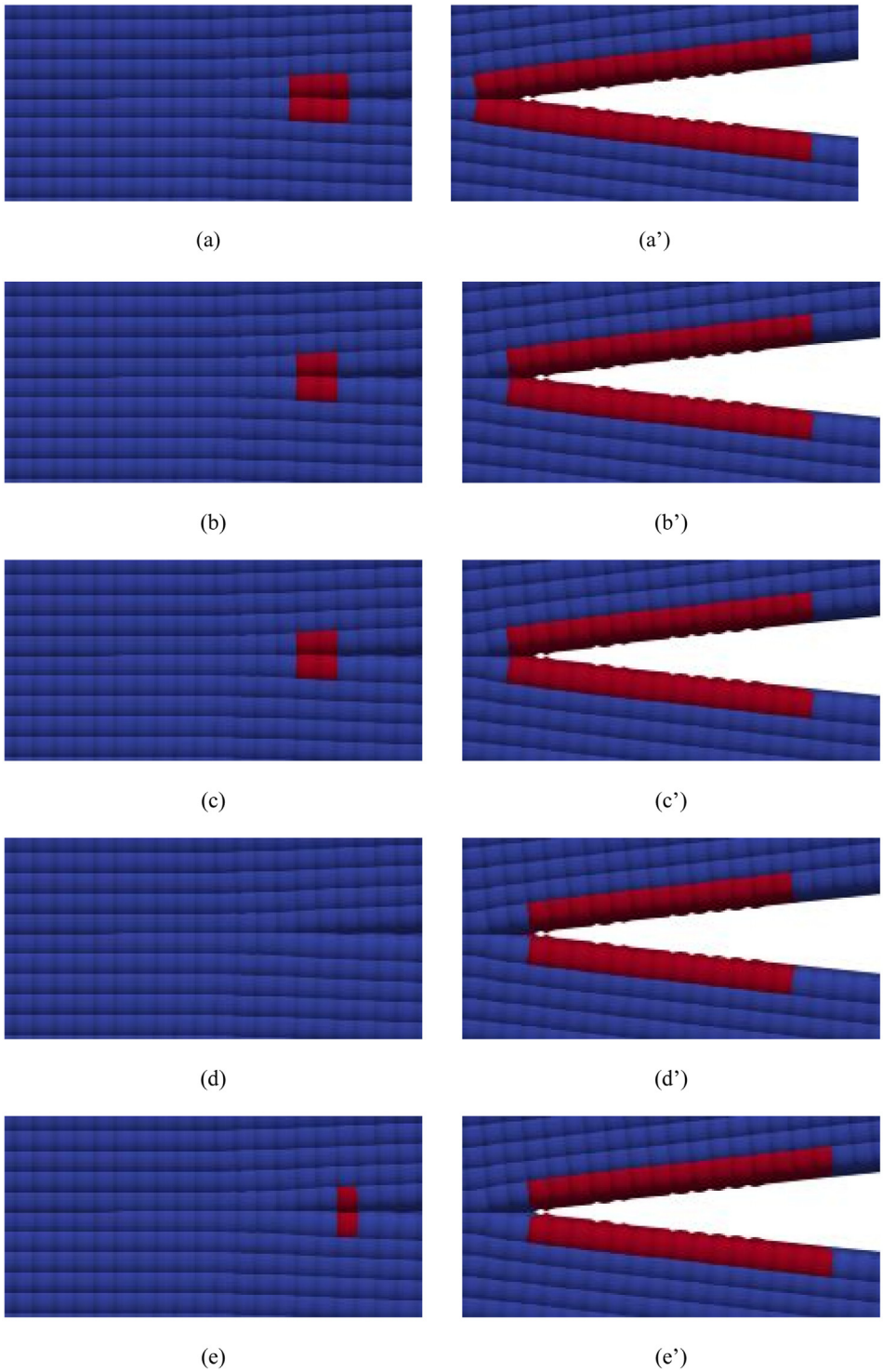

Fig. 4. Crack propagation at 32k and 59k cycles, respectively, (a)(a') nodal damage value of 0.3 (b)(b') nodal damage value of 0.35 (c)(c') nodal damage value of 0.4 (d)(d') nodal damage value of 0.45 (e)(e') the proposed method.

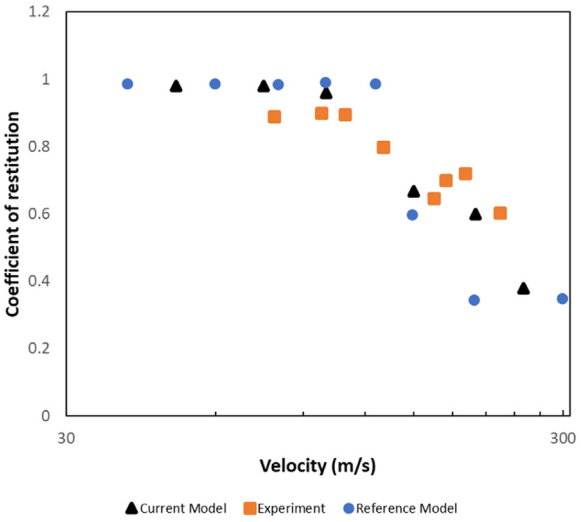

Fig. 5. A comparison between the data in [40] and the model proposed by the current paper.

with modulus of elasticity of 115 GPa and fracture energy of 2.665 kJ/m^2. The density and Poisson's ratio values are not mentioned in the referred study. Those values are obtained from [41,42].

In [40], the model was verified with an experiment [43] in terms of coefficient of restitution (C_r). Similarly, Fig. 5 compares the current model, the referred model and the experiment presented in [40]. As can be seen from the figure, the pattern of current model follows the behaviour of the experiment and the model. The value of C_r remains constant below 100 m/s, which is close to 1, indicating that collision is perfectly elastic with no energy dissipation. At higher velocities, the ball starts to lose some of its energy and therefore, the value of C_r decreases.

To show the effect of various nodal damage values, crack propagation speeds are measured for four different crack paths, similar to referred study. Selected paths are presented in Fig. 6a. It is noteworthy that crack paths are symmetric due to symmetric discretization and symmetrically applied force since the ball centre and plate centre are colinear. Fig. 6b-e give the crack propagation speed for North, Northeast, Southeast and West crack paths. The measurements are given in radial distance with respect to micro seconds. The formula to calculate crack velocity is given in Eq. (20).

$$v = 1/N \sum_{N} ((d_f - d_i)/(t_f - t_i)) \tag{20}$$

where v, d, t, f, i, N represent average velocity, distance, time, final value, initial value and number of crack paths, respectively. From Fig. 6b-e, it is perceptible that there is a negative correlation between nodal damage value and crack speed. The lower the nodal damage value is, the higher is the crack speed. Thus, the correct assignment of nodal damage value becomes more crucial in impact problems. It is obvious that the same simulation produce significantly different results with respect to nodal damage value. On the other hand, the proposed method is independent from nodal damage value and gives a single value for the crack propagation speed Fig. 6f. The crack speed of 1217 m/s for the proposed method is relatively lower than crack propagation speeds for nodal damage values. The closer investigation in the simulation environment provides two explanations. First, the nodal damage value produce different the crack propagation speeds. It is likely that higher nodal damage value can produce lower crack propagation speed. Secondly, it is observed that two cracks merge on the same path when the proposed method is used or the nodal damage value is high. The result of this behaviour can be seen in Fig. 6e, where Northeast and West cracks slowly propagates between 4 and 8 μs on the contrary to North and Southeast cracks which show a jump at 8 μs.

The visual assessments of the proposed method and nodal damage value can provide more insight into the problem. In Fig. 7a, the plate from the simulation is presented after magnifying displacement field by 500x and application of cut-off filter with damage value of 0.85 that filters out free nodes and severely damaged nodes. Then, the points having nodal damage values in Fig. 6 are also filtered out to present clear picture for the corresponding damage value. Fig. 7b-e illustrates crack propagation associated with different nodal damage values after filtering out damaged nodes above nodal damage values. It is apparent from Fig. 7b-d that those damage values,0.3–0.5, clearly overestimates the crack propagation since a concentric separation between outer and inner part exist and there are a lot of chunks in the inner part when compared to Fig. 7a. Fig. 7e has no concentric separation between inner and outer part and therefore, nodal damage value of 0.6 is relatively accurate to estimate crack propagation even though the ratio of the damaged area to undamaged area seems to be higher in comparison to Fig. 7a. In Fig. 7f, the illustration of proposed method is presented. As can be seen from the figure, the proposed method captures large cracks clearly. By looking at Fig. 7a closely, one may claim that perceptible shallow cracks in Fig. 7a are not captured by the proposed method. It should be emphasized that the displacement field is magnified

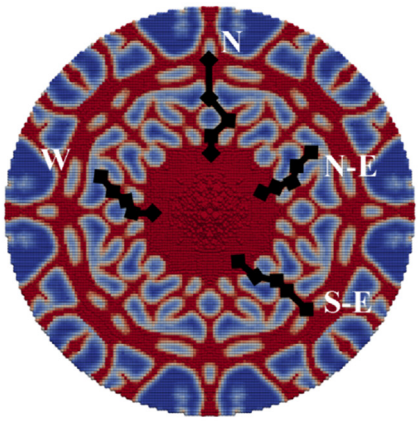

(a)

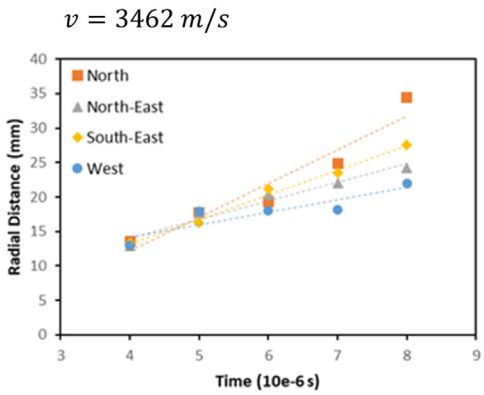

(b)

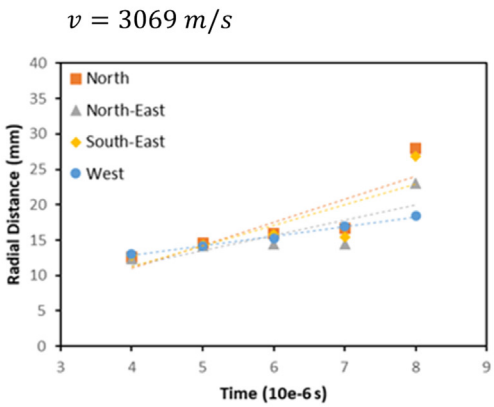

(c)

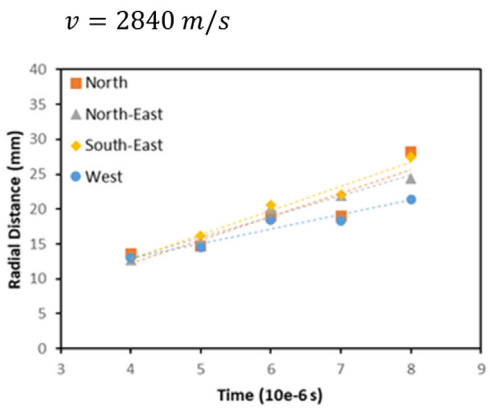

(d)

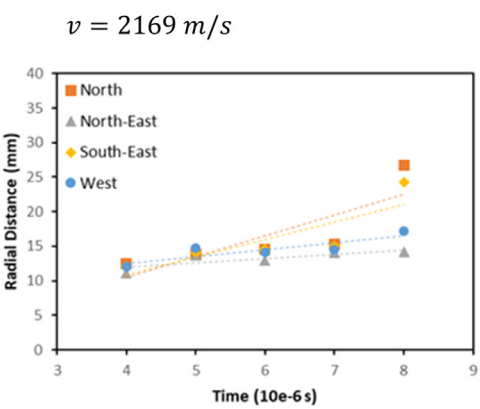

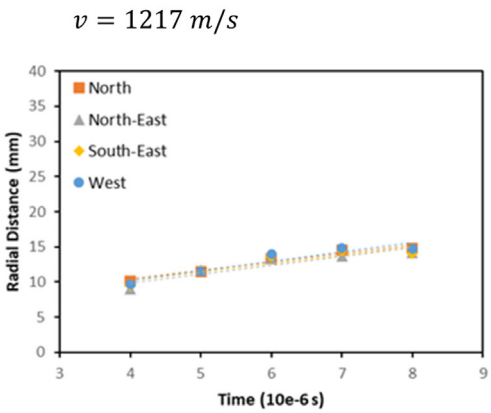

Fig. 6. Crack propagation speed on four different paths (a) selected paths (b) the nodal damage of 0.3 (c) the nodal damage of 0.4 (d) the nodal damage of 0.5 (e) the nodal damage of 0.6 (f) the proposed method.

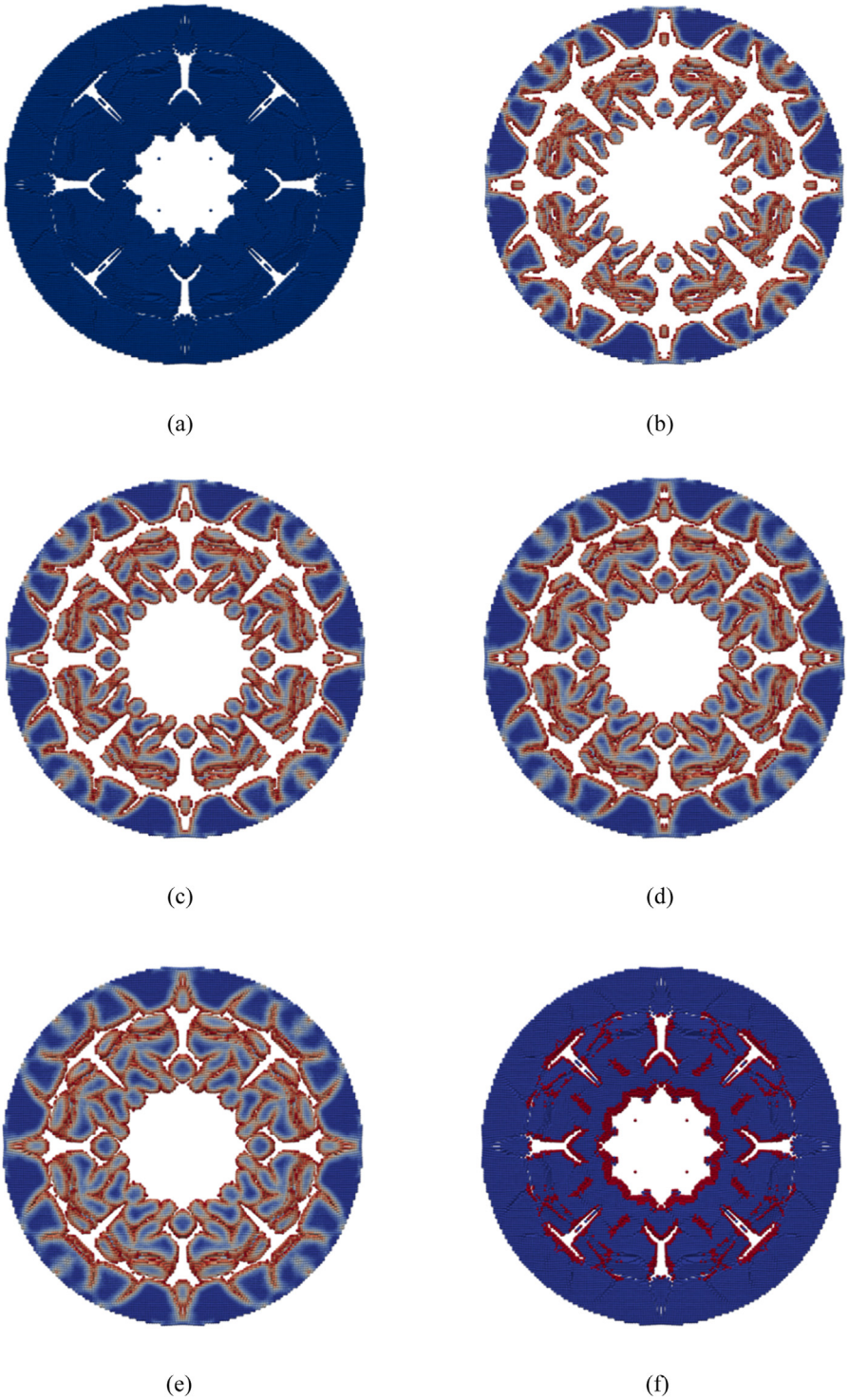

Fig. 7. Crack profiles (a) Free from any methods (b) the nodal damage of 0.3 (c) the nodal damage of 0.4 (d) the nodal damage of 0.5 (e) the nodal damage of 0.6 (f) the proposed method.

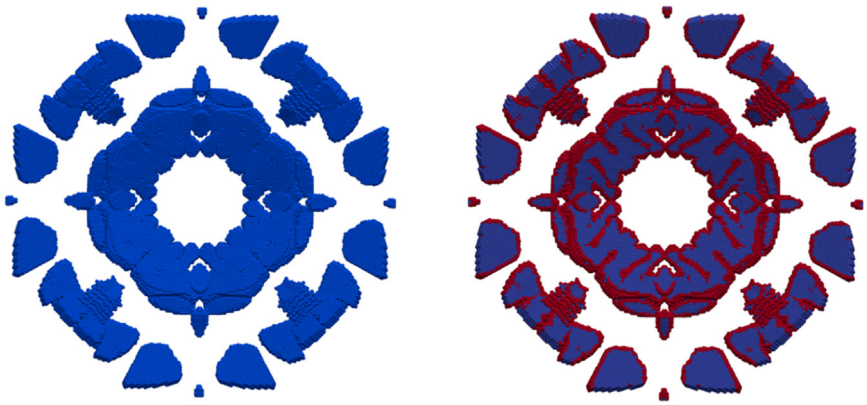

Fig. 8. Crack profiles (a) Free from any methods (b) the proposed method.

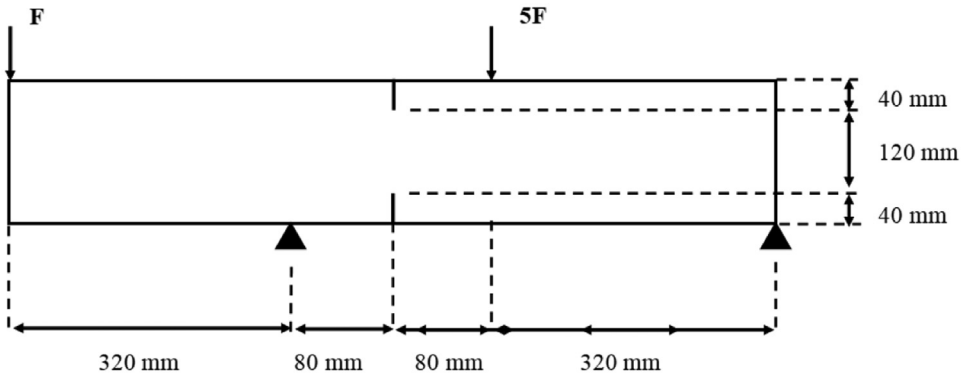

Fig. 9. The dimensions of concrete specimen.

by 500x, which enables to see those separations on the surface. Nevertheless, it does not mean all the bonds between neighbouring nodes are broken. In other words, the propagation condition of the proposed method is not satisfied. To ensure the sufficiency of the method, Fig. 8 is presented with a magnification factor of 100x that is applied to displacement. In Fig. 8b, it is apparent that the proposed method captures all the cracks in Fig. 8a.

3.3. Case 3 – crack propagation in a double-edge notched concrete

The experiment of the double edge notched concrete under loading [44] has been used in various studies [45–47] as a reference to validate the numerical models of crack propagation in concrete structure. It is a classical failure problem with a simple configuration. To demonstrate the capability of proposed method, the same setup is simulated in Peridynamics (PD) with an exception of that the simulation is conducted in two steps. In the first step, the quasi-static solver is used to find the equilibrium before crack propagation. Then, explicit solver is activated to solve the crack propagation problem with a small increments that yield close to quasi-static solution (maximum strain rate $<$ 1.0e-4) until failure which is absolutely dynamic. The idea behind of two-step is to reduce the simulation time and apply similar conditions to experimental method, which was quasistatic. It is noteworthy that quasi-static solutions of PD involve some challenges related to the nature of crack problem as well as PD itself [48].

Fig. 9 illustrates the dimensions of the beam specimen with a modulus of elasticity of 27 GPa, density of 2400 kg/m3, Poisson's ratio of 0.18 and mode-I fracture energy of 100 N/m. The crack depth is 40 mm and the load increases from 0 to 47.6 kN, gradually and slowly. The geometry is discretised into points that are equally distanced in 0.5 mm, resulting in 128k nodes. The PD parameter of horizon is 15 mm ($3\Delta x$) with reference to recommendation in [1].

In Fig. 10a, the PD model of the concrete specimen shows fair agreement to the experiment. Though, the PD model overestimates the failure point, where a snap-back occurs. The discrepancy could result from PD parameters as well as the nature of the failure itself. The experimental and PD failure modes are illustrated in Fig. 10b-d. As can be seen from the figures, PD simulation exhibits similar failure modes to the experiment. Nevertheless, the curvature of the crack paths in PD simulation is relatively lower than the experiment, associated with relatively large mesh size. In Fig. 10c-d, the maximum strain before and after failure is presented to show the potential crack path as well as strain relief following the failure. In

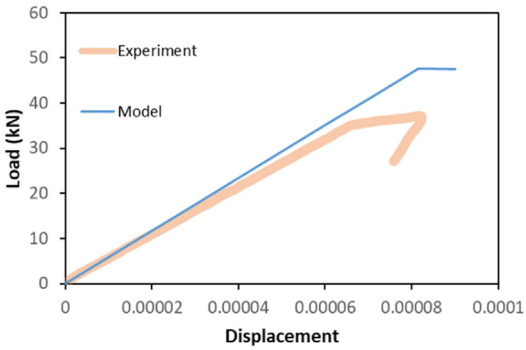

(a)

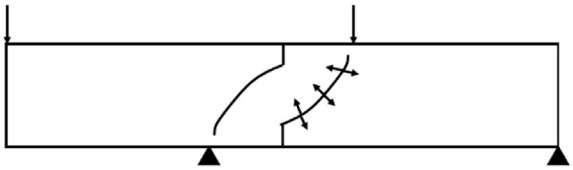

(b)

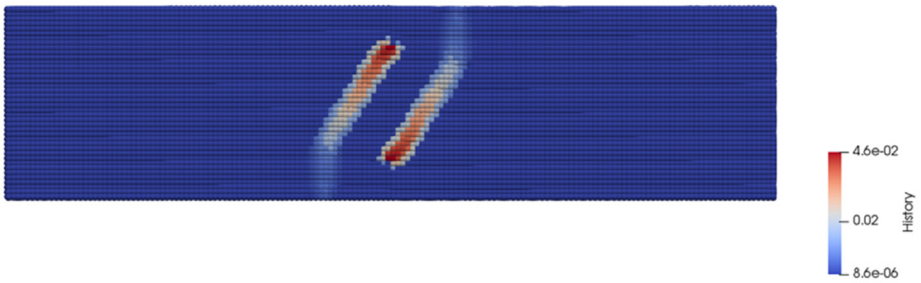

(c)

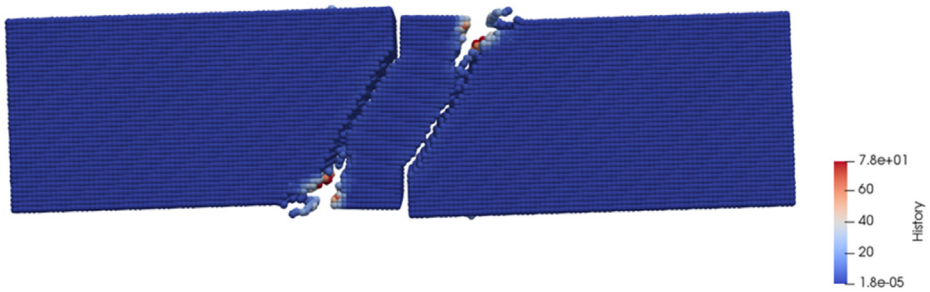

(d)

Fig. 10. (a) Comparison between experiment and model (b) the failure mode presented in [44] (c) maximum strains before failure (d) maximum strains after failure.

the figures, the area with dense red points are the crack tips of the bottom and top notches. Likewise, the area with light blue points represents the force points.

As aforementioned, Fig. 11 that is captured just before the failure proves that the magnitude of the nodal damage value to represent crack propagation is decisive on how the crack forms. In the figure, the damage values below the threshold nodal damage value are filtered out. Similarly, the damage values above the threshold are also painted with same colour of threshold value to present a clear picture. As Fig. 11a-d show, there is a significant difference between crack paths of various nodal damage values. The lower nodal damage values estimate large and apparent crack paths and it is vice versa for the higher values. On the other side, the proposed method estimates a partial crack propagation. In comparison to nodal damage value of 0.3, the proposed method indicates that the straight part of the crack path that is under the force acting points has not appeared, yet. Lastly, the crack path formation after clear failure is presented in Fig. 12. Apparently, the higher nodal damage value cannot estimate the crack path accurately, in the case of four point bending of double edge notched concrete sample. The lowest value of average damage and proposed method exhibit similar behaviour after failure. It might be said that ideal value of average damage is 0.3 in the case of quasi-static mixed mode failure in addition to proposed method.

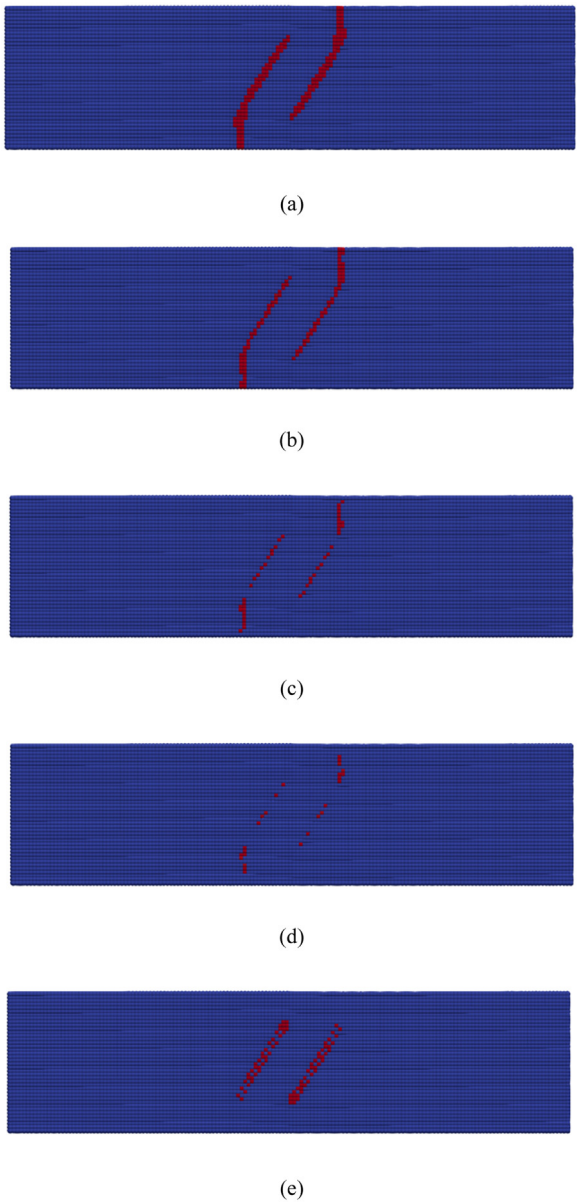

Fig. 11. Crack path estimation with respect to nodal damage values and the proposed method before the apparent failure (a) the nodal damage of 0.3 (b) the nodal damage of 0.4 (c) the nodal damage of 0.5 (d) the nodal damage of 0.6 (e) the proposed method.

Nevertheless, the nodal damage value of 0.3 lose its validity in dynamic and fatigue problems, which was presented in the previous sections.

3.4. Case 4 – dynamic crack propagation

The fourth case to investigate the advantage of the proposed method involves crack growth with branching. For this purpose, the simulation in [49] is repeated here. The geometry of the specimen, which is pre-notched glass sheet, is illustrated in Fig. 13a. The specimen has the modulus of elasticity of 32 GPa, a Poisson's ratio of 0.2 and a density of 2450 kg/m^3. A tensile stress with a magnitude of 1 MPa is applied at top and bottom surfaces. The geometry consists of points that is equally distanced by 0.5 mm in x, y, z, directions . The horizon parameter of 1.5 mm is applied in the simulations.

It was mentioned in [49] with reference to the experimental study [50] that crack propagates on a straight path with a gradually increasing speed and then, after exceeding a certain speed value, it splits into at least two different cracks.

The experimental observation and the outcome of numerical simulation (conducted with Extended Finite Element Method (XFEM)) in [49] are presented in Fig. 13b-c. As shown in Fig. 13d, the outcome of the proposed method also follows

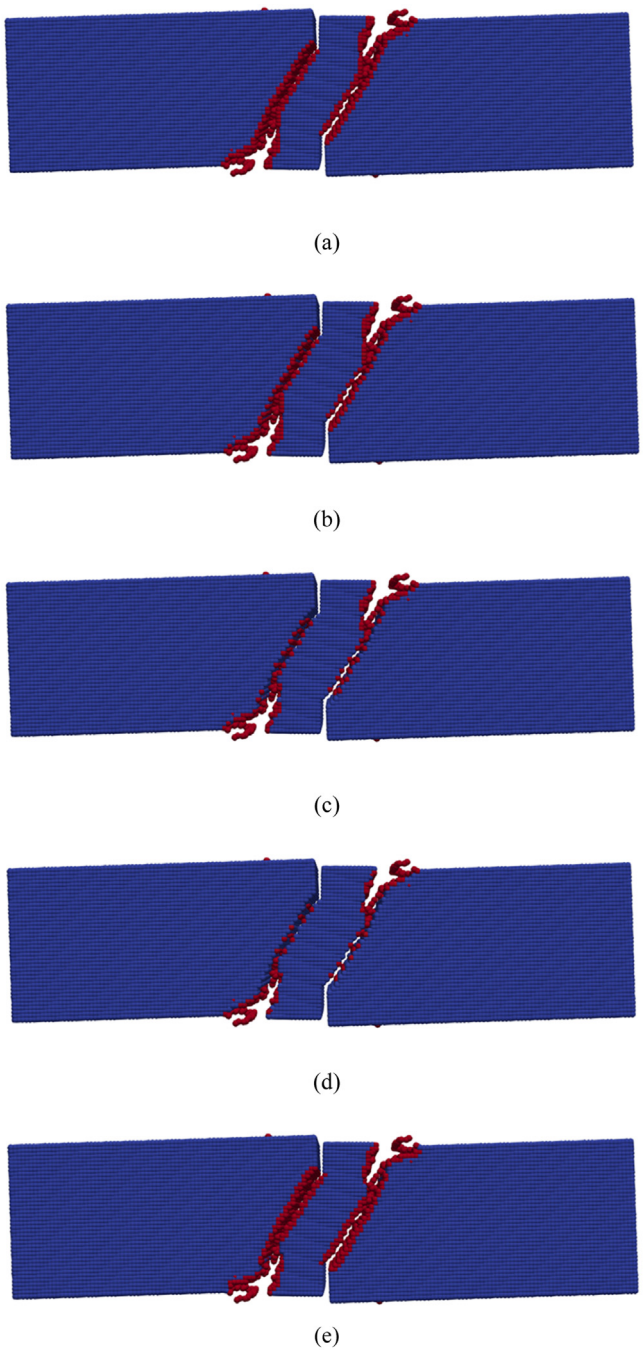

Fig. 12. Crack path estimation with respect to nodal damage values and the proposed method after the apparent failure (a) the nodal damage of 0.3 (b) the nodal damage of 0.4 (c) the nodal damage of 0.5 (d) the nodal damage of 0.6 (e) the proposed method.

a similar trend in general. The crack first propagates on a straight line and then, at certain point, it splits into two different cracks. A perceptible difference is related to the estimation of minor cracks prior to crack split, which were observed in the experiment but underestimated by Peridynamics (PD) as well as XFEM. It is noteworthy that the application of nodal damage values also gives same crack paths. Therefore, only the result of proposed method is presented in Fig. 13.

The crack propagation speeds obtained by different methods are compared in Fig. 14. The methods used in [49] are shown in orange colour. Likewise, different nodal damage values and proposed method are depicted in blue and green colours, respectively. It is apparent in the figure that PD estimation of crack propagation speed is between interelement method and XFEM, which provides a confidence in estimating crack propagation and branching. What is interesting in

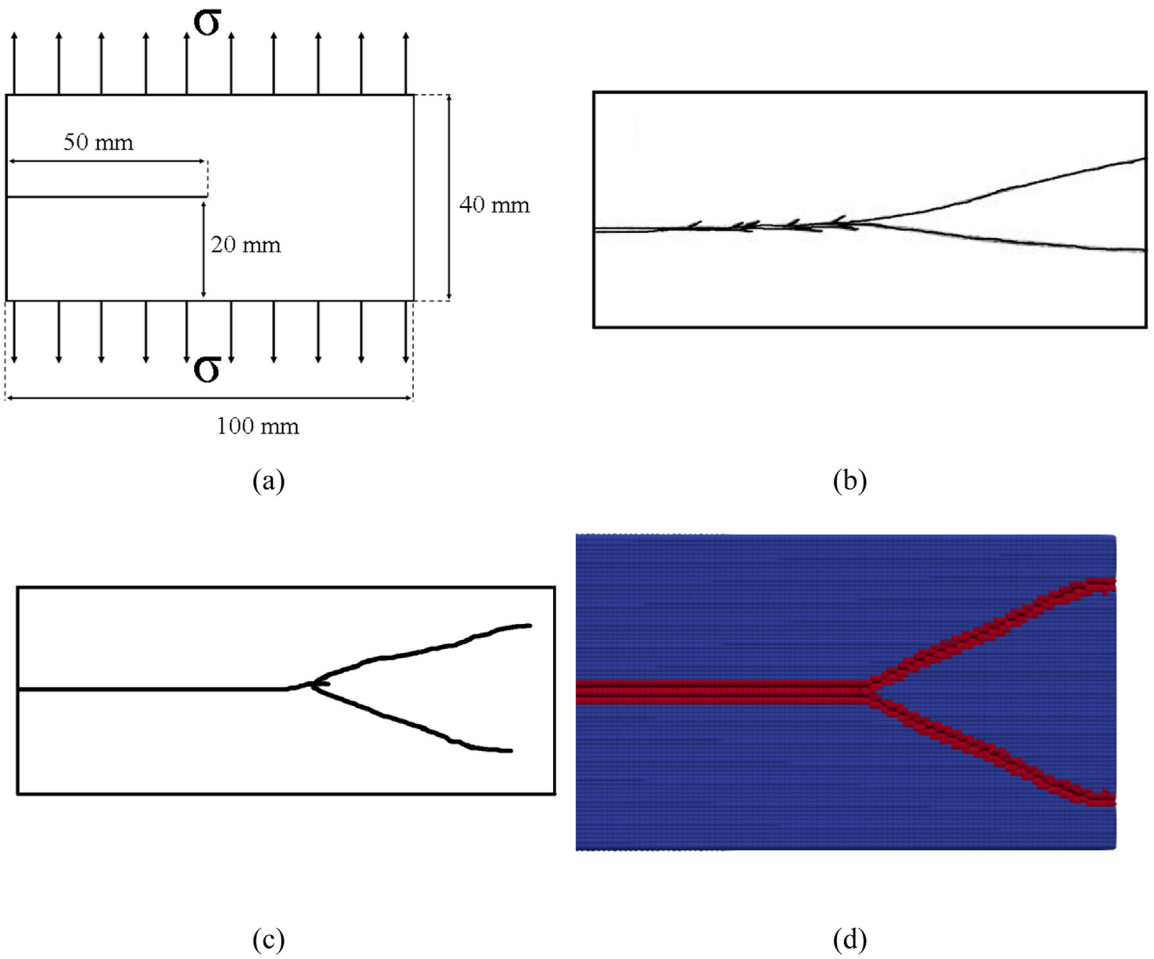

Fig. 13. (a) The illustration of the specimen (b) the sketch of experimental result (KOBAYSHI) (c) the sketch of XFEM result (SONG) (d) the result of the proposed method.

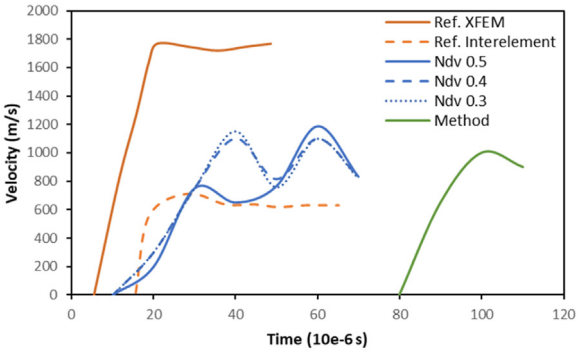

Fig. 14. Crack propagation speeds estimated by different methods.

Fig. 14 is that the proposed method estimates the start of crack propagation far beyond the start points provided by the other methods, which might disprove the proposed method. Hence, this contradictory outcome is investigated further. It should be reminded that PD theory is established on the interactions of nodes or so-called bond's behaviour. A loss of interactions, namely broken bonds, defines the damage. In many studies, it is assumed that a nodal damage value is sufficient to determine the number of bonds of a point that must be broken to assume that there is a damage in the vicinity of that point. Even though this assumption seems to be independent from damage location, it takes that information into account indirectly. In those studies, the nodal damage value represents the number of bonds belonging to the damaged side of the

point, figuratively. As aforementioned, there are limited number of studies in which the number of bonds passing through a crack path that must be broken is manually calculated. In those studies, if a single bond passing through crack surface is still intact at specific location, then the crack at that location does not exist yet.

To verify the proposed method or to explain the reason why the proposed method estimated the late start propagation, it is imperative to track the condition of the relevant bonds. If there is any non-broken bonds that pass through the crack path(used in the previous studies) or the mid-plane (offered by current method), it means that nodal damage value ignores the existence of some non-broken bonds. It is worth mentioning that the crack path and mid-plane have similar orientation and location for the straight part of the crack in the current example. To examine the condition of the relevant bonds, two points on the crack path are selected. Selected two points are located in Fig. 15a-c. The detailed neighbour information and non-broken bonds of the common neighbours for the selected points are given in Fig. 15d-f for different time steps(i.e. 40, 100,110 microseconds). In the figures, red and blue dots are the selected points. Red and blue crosses are the unique neighbours of corresponding points and black crosses represent common neighbours of those two points. The crack path and mid-plane lays between the selected two nodes. As shown in Fig. 15e, there are several non-broken bonds that pass through crack path. With reference to the concept of PD bonds, it can be concluded that the damage has not occurred yet. Moreover, nodal damage values neglect non-broken bonds in that case. In other words, Fig. 15e reveals that the failure criteria of proposed method have not yet met, which yields the late start of crack propagation. Considering the similarities and discrepancies in Fig. 14, one may suggest to use nodal damage values to evaluate damage with a cost of ignoring some non-broken bonds. In that case, the nonlocality of PD theory might become questionable.

4. Discussions

Since there is no consensus on how to determine the nodal damage value, most of the studies are interpreted by visual assessments. In the other few studies, several attempts have been made to quantify the damage. Nevertheless, those studies have significant drawbacks which were underlined previously in the introduction. As shown throughout this paper, selection of the nodal damage value significantly influence the results. The uniqueness of the study is to set a robust condition that enables to produce a single outcome for any simulation whereas nodal damage value can produce multiple outcomes associated with the magnitude of nodal damage value. This paper proposes that the damage will occur when all direct and first degree indirect contacts between two closest neighbour are lost. The proposed method is offered with a consideration of the non-local nature of PD theory.

It should be emphasized that visual assessment of the PD simulations by nodal damage value could be indicative in quasi-static simulations at some degree when the crack evolution is ignored. Furthermore, the value could be determined to certain degree by using so-called bond filters that ignores any bond passing through a crack plane and can assist to figure out the number of ignored bonds to calculate nodal damage value. Nevertheless, the results of the simulations show that those approaches fails in dynamic and fatigue problems where crack propagation speed is crucial.

One may question the advantage of the proposed method in fatigue case where the extraction of the material constants can also be done with reference to nodal damage value. However, it is noteworthy that those constants could also be produced for irrelevant values such as nodal damage value of 0.01, which means a few broken bonds could reflect the crack propagation behaviour. On the other hand, the proposed method removes some parts of the virtuality of the fatigue model. Indeed, it is believed that there must be correlation between proposed method and crack propagation since it defines the propagation in more physical way. Hence, it is aimed to conduct further studies to figure out the relation between proposed method and crack propagation. The proposed method might be capable of simulating the crack initiation part of the applied fatigue model. Crack initiation was mentioned several times in many studies but never investigated thoroughly due to the challenge in setting and verifying the condition that will initiate the crack.

It is worth mentioning that proposed method could be computationally expensive due to the number of subsets of the direct and indirect neighbour points. Hence, it is preferred to apply specific conditions that decrease the simulation time. This paper also proposes that damage will occur on a mid-plane of two neighbouring points when all the bonds of those two neighbours that pass through the plane are broken. Moreover, the plane will occur when the direct contact is lost. Currently, the cost of computation seems to be reasonable to use the current methodology of crack-on-midplane. The proposed method is vastly applicable to various engineering structures under dynamic and impact loading conditions such as rail surface defacts [20], railway switches and crossings [51], and so on.

5. Conclusions

The main aim of this paper is to propose a new methodology to assess the damage initiation and propagation in Peridynamics (PD) simulations. Currently, the damage assessment is mostly based on the nodal damage value the magnitude of which shows variations within the literature. Therefore, outcomes of the simulations concerning the nodal damage value become subjective and the impact of this subjectivity has been presented throughout this paper.

This paper proposes a new philosophy “the damage will occur when all direct and first degree indirect contacts between two closest neighbour are lost” for damage assessments and a new method associated with that philosophy. The method sets an objective criterion and yields a single outcome while showing crack formations.

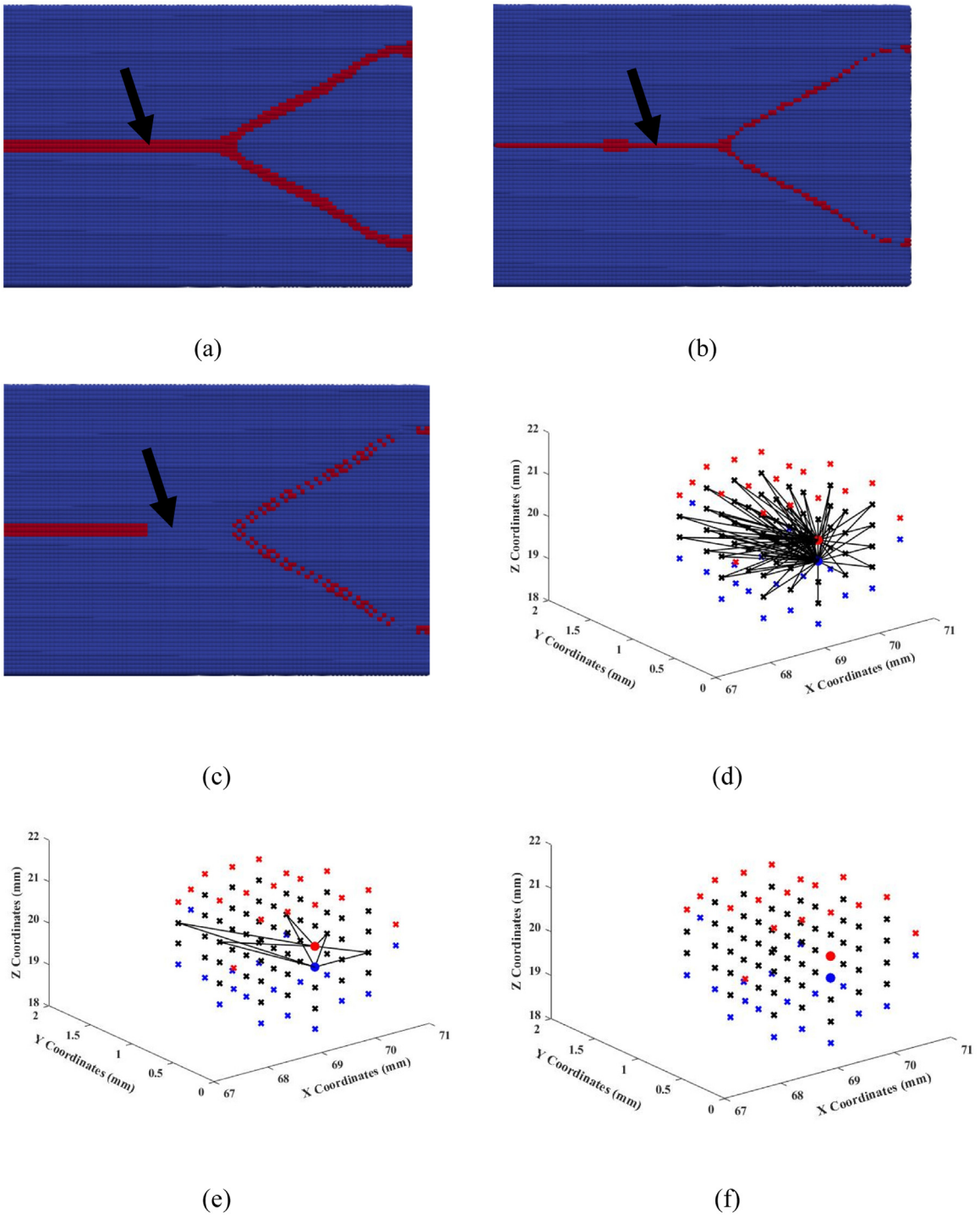

Fig. 15. Crack propagation at 100 microseconds for (a) NDV of 0.3 (b NDV of 0.5 (c) the proposed method. The bond conditions of selected points (d) at 40 microseconds (e) at 100 microseconds (f) at 110 microseconds.

In conclusion, in this paper, a comparison between the nodal damage value and the new method has been presented for four cases. The new method appears to be rigorously effective and relatively efficient tool to trace the crack propagation and initiation. More importantly, it does not produce different results in the same simulation. Further studies will be conducted to test the range of validity and the cost of computation for proposed method in various scenarios.

Declaration of Competing Interest

The authors declare that they have no known competing financial interests or personal relationships that could have appeared to influence the work reported in this paper.

Data availability

Data will be made available on request.

Acknowledgments

The first author would like to gratefully acknowledge the sponsorships and assistance from Ministry of National Education (Turkey). We also wish to gratefully acknowledge European Commission for H2020-MSCA-RISE Project No. 691135 “RISEN: Rail Infrastructure Systems Engineering Network” (www.risen2rail.eu) and for partial support from H2020 Shift2Rail Project No 730849 (S-Code). The technical sponsorships and assistance from China Academy of Railway Sciences, Japan Railway Technical Research Institute, Network Rail, RSSB (Rail Safety and Standard Board, UK) are appreciated.

References

[1] E. Madenci, E. Oterkus, in: Peridynamic Theory and Its Applications, Springer, 2014, pp. 19–43, doi:10.1007/978-1-4614-8465-3.
[2] M. Kuna, Finite Elements in Fracture Mechanics, 10, Springer, 2013, doi:10.1007/978-94-007-6680-8.
[3] N. Moës, J. Dolbow, T. Belytschko, A finite element method for crack growth without remeshing, Int. J. Numer. Methods Eng. 46 (1) (1999) 131–150, doi:10.1002/(SICI)1097-0207(19990910)46:1<131::AID-NME726>3.0.CO;2-J.
[4] S.A. Silling, Reformulation of elasticity theory for discontinuities and long-range forces, J. Mech. Phys. Solids 48 (1) (2000) 175–209, doi:10.1016/S0022-5096(99)00029-0.
[5] S.A. Silling, M. Epton, O. Weckner, J. Xu, E. Askari, Peridynamic states and constitutive modeling, J. Elast. 88 (2) (2007) 151–184, doi:10.1007/s10659-007-9125-1.
[6] T.L. Warren, S.A. Silling, A. Askari, O. Weckner, M.A. Epton, J. Xu, A non-ordinary state-based peridynamic method to model solid material deformation and fracture, Int. J. Solids Struct. 46 (5) (2009) 1186–1195, doi:10.1016/j.ijsolstr.2008.10.029.
[7] M.R. Tupek, R. Radovitzky, An extended constitutive correspondence formulation of peridynamics based on nonlinear bond-strain measures, J. Mech. Phys. Solids 65 (2014) 82–92, doi:10.1016/j.jmps.2013.12.012.
[8] R. Delorme, P. Diehl, I. Tabiai, L.L. Lebel, M. Lévesque, Extracting constitutive mechanical parameters in linear elasticity using the virtual fields method within the ordinary state-based peridynamic framework, J. Peridyn. Nonlocal Model. 2 (2020) 111–135, doi:10.1007/s42102-019-00025-7.
[9] E. Madenci, M. Dorduncu, N. Phan, X. Gu, Weak form of bond-associated non-ordinary state-based peridynamics free of zero energy modes with uniform or non-uniform discretization, Eng. Fract. Mech. 218 (2019) 106613, doi:10.1016/j.engfracmech.2019.106613.
[10] P. Diehl, R. Lipton, T. Wick, Tyagi, A comparative review of peridynamics and phase-field models for engineering fracture mechanics, Comput. Mech. 69 (2022) 1259–1293, doi:10.1002/nme.6542.
[11] D. Huang, G. Lu, P. Qiao, An improved peridynamic approach for quasi-static elastic deformation and brittle fracture analysis, Int. J. Mech. Sci. 94 (2015) 111–122, doi:10.1016/j.ijmecsci.2015.02.018.
[12] M.S. Breitenfeld, P.H. Geubelle, O. Weckner, S.A. Silling, Non-ordinary state-based peridynamic analysis of stationary crack problems, Comput. Methods Appl. Mech. Eng. 272 (2014) 233–250, doi:10.1016/j.cma.2014.01.002.
[13] B. Kilic, E. Madenci, Prediction of crack paths in a quenched glass plate by using peridynamic theory, Int. J. Fract. 156 (2) (2009) 165–177, doi:10.1007/s10704-009-9355-2.
[14] F. Bobaru, M. Duangpanya, The peridynamic formulation for transient heat conduction, Int. J. Heat Mass Transf. 53 (19–20) (2010) 4047–4059, doi:10.1016/j.ijheatmasstransfer.2010.05.024.
[15] Y.D. Ha, F. Bobaru, Studies of dynamic crack propagation and crack branching with peridynamics, Int. J. Fract. 162 (1) (2010) 229–244, doi:10.1007/s10704-010-9442-4.
[16] Z. Cheng, Y. Liu, J. Zhao, H. Feng, Y. Wu, Numerical simulation of crack propagation and branching in functionally graded materials using peridynamic modeling, Eng. Fract. Mech. 191 (2018) 13–32, doi:10.1016/j.engfracmech.2018.01.016.
[17] Silling, S.A. and Askari A., Peridynamic model for fatigue cracking. SAND2014-18590. Albuquerque: Sandia National Laboratories, 2014. 10.2172/1160289
[18] J. Jung, J. Seok, Mixed-mode fatigue crack growth analysis using peridynamic approach, Int. J. Fatigue 103 (2017) 591–603, doi:10.1016/j.ijfatigue.2017.06.008.
[19] C.T. Nguyen, S. Oterkus, E. Oterkus, An energy-based peridynamic model for fatigue cracking, Eng. Fract. Mech. 241 (2021) 107373, doi:10.1016/j.engfracmech.2020.107373.
[20] A. Freimanis, S. Kaewunruen, Peridynamic analysis of rail squats, Appl. Sci. 8 (11) (2018) 2299, doi:10.3390/app8112299.
[21] J.A. Mitchell, A non-local, ordinary-state-based viscoelasticity model for peridynamics, Sandia Natl. Lab Rep. 8064 (2011) 1–28, doi:10.2172/1029821.
[22] J.T. Foster, S.A. Silling, W.W. Chen, Viscoplasticity using peridynamics, Int. J. Numer. Methods Eng. 81 (10) (2010) 1242–1258, doi:10.1002/nme.2725.
[23] Y. Gao, S. Oterkus, Fully coupled thermomechanical analysis of laminated composites by using ordinary state based peridynamic theory, Compos. Struct. 207 (2019) 397–424, doi:10.1016/j.compstruct.2018.09.034.
[24] E. Askari, F. Bobaru, R.B. Lehoucq, M.L. Parks, S.A. Silling, O. Weckner, Peridynamics for multiscale materials modeling, J. Phys. Conf. Ser. (2008), doi:10.1088/1742-6596/125/1/012078.
[25] W. Liu, J.W. Hong, A coupling approach of discretized peridynamics with finite element method, Comput. Methods Appl. Mech. Eng. 245 (2012) 163–175, doi:10.1016/j.cma.2012.07.006.
[26] T. Ni, M. Zaccariotto, Q. Zhu, U. Galvanetto, Coupling of FEM and ordinary state-based peridynamics for brittle failure analysis in 3D, Mech. Adv. Mater. Struct. 28 (9) (2021) 875–890, doi:10.1080/15376494.2019.1602237.
[27] Q. Le, F. Bobaru, Surface corrections for peridynamic models in elasticity and fracture, Comput. Mech. 61 (4) (2018) 499–518, doi:10.1007/s00466-017-1469-1.

[28] S. Shen, Z. Yang, F. Han, J. Cui, J. Zhang, Peridynamic modeling with energy-based surface correction for fracture simulation of random porous materials, Theor. Appl. Fract. Mech. 114 (2021) 102987, doi:10.1002/nme.5257.
[29] A. Javili, R. Morasata, E. Oterkus, S. Oterkus, Peridynamics review, Math. Mech. Solids 24 (11) (2019) 3714–3739 10.1177%2F1081286518803411.
[30] E. Madenci, S. Oterkus, Ordinary state-based peridynamics for plastic deformation according to von Mises yield criteria with isotropic hardening, J. Mech. Phys. Solids 86 (2016) 192–219, doi:10.1016/j.jmps.2015.09.016.
[31] L. Wu, D. Huang, Y. Xu, L. Wang, A rate-dependent dynamic damage model in peridynamics for concrete under impact loading, Int. J. Damage Mech. 29 (7) (2020) 1035–1058 10.1177%2F1056789519901162.
[32] H. Zhang, P. Qiao, A state-based peridynamic model for quantitative fracture analysis, Int. J. Fract. 211 (1) (2018) 217–235, doi:10.1007/s10704-018-0285-8.
[33] J. Schijve, Fatigue of Structures and Materials, Springer Science & Business Media, 2001, doi:10.1007/978-1-4020-6808-9.
[34] N. Zhu, C. Kochan, E. Oterkus, S. Oterkus, Fatigue analysis of polycrystalline materials using Peridynamic theory with a novel crack tip detection algorithm, Ocean Eng. 222 (2021) 108572, doi:10.1016/j.oceaneng.2021.108572.
[35] M.L. Parks, D.J. Littlewood, J.A. Mitchell, S.A. Silling, Peridigm Users' Guide v1. 0.0, SAND Report (2012) 7800, doi:10.2172/1055619.
[36] R.M. Nejad, M. Shariati, K. Farhangdoost, Prediction of fatigue crack propagation and fractography of rail steel, Theor. Appl. Fract. Mech. 101 (2019) 320–331, doi:10.1016/j.tafmec.2019.03.016.
[37] International, A., ASTM E647-standard test method for measurement of fatigue crack growth rates, 2015: West Conshohocken, PA. 10.1520/E0647-15
[38] F. Scabbia, M. Zaccariotto, U. Galvanetto, A novel and effective way to impose boundary conditions and to mitigate the surface effect in state-based Peridynamics, Int. J. Numer. Methods Eng. 122 (20) (2021) 5773–5811, doi:10.1002/nme.6773.
[39] M.J. Dai, S. Tanaka, P. Guan, S. Oterkus, E. Oterkus, Ordinary state-based peridynamic shell model with arbitrary horizon domains for surface effect correction, Theor. Appl. Fract. Mech. 115 (2021) 103068, doi:10.1016/j.tafmec.2021.103068.
[40] J. Rivera, J. Berjikian, R. Ravinder, H. Kodamana, S. Das, N. Bhatnagar, M. Bauchy, N.M. Anoop Krishnan, Glass fracture upon ballistic impact: new insights from peridynamics simulations, Front. Mater. 6 (2019) 239, doi:10.3389/fmats.2019.00239.
[41] F. Bobaru, Y.D. Ha, W. Hu, Damage progression from impact in layered glass modeled with peridynamics, Cent. Eur. J. Eng. 2 (4) (2012) 551–561, doi:10.2478/s13531-012-0020-6.
[42] http://www.mit.edu/~6.777/matprops/copper.htm. 2021 [cited 2021 04/11].
[43] C. Knight, M.V. Swain, M. Chaudhri, Impact of small steel spheres on glass surfaces, J. Mater. Sci. 12 (8) (1977) 1573–1586, doi:10.1007/BF00542808.
[44] P. Bocca, A. Carpinteri, S. Valente, Size effects in the mixed mode crack propagation: softening and snap-back analysis, Eng. Fract. Mech. 35 (1–3) (1990) 159–170, doi:10.1016/0013-7944(90)90193-K.
[45] D. Huang, G. Lu, Y. Liu, Nonlocal peridynamic modeling and simulation on crack propagation in concrete structures, Math. Probl. Eng. 2015 (2015) 1–11, doi:10.1155/2015/858723.
[46] T. Rabczuk, T. Belytschko, Cracking particles: a simplified meshfree method for arbitrary evolving cracks, Int. J. Numer. Methods Eng. 61 (13) (2004) 2316–2343, doi:10.1002/nme.1151.
[47] M. Zaccariotto, F. Luongo, U. Galvanetto, Examples of applications of the peridynamic theory to the solution of static equilibrium problems, Aeronaut. J. 119 (1216) (2015) 677–700, doi:10.1017/S0001924000010770.
[48] B. Kilic, E. Madenci, An adaptive dynamic relaxation method for quasi-static simulations using the peridynamic theory, Theor. Appl. Fract. Mech. 53 (3) (2010) 194–204, doi:10.1016/j.tafmec.2010.08.001.
[49] J.H. Song, H. Wang, T. Belytschko, A comparative study on finite element methods for dynamic fracture, Comput. Mech. 42 (2) (2008) 239–250, doi:10.1007/s00466-007-0210-x.
[50] M. Ramulu, A. Kobayashi, Mechanics of crack curving and branching—a dynamic fracture analysis, Dyn. Fract. (1985) 61–75, doi:10.1007/978-94-009-5123-5_5.
[51] M. Hamarat, M. Papaelias, S. Kaewunruen, Fatigue damage assessment of complex railway turnout crossings via Peridynamics-based digital twin, Sci. Rep. 12 (1) (2022) 14377, doi:10.1038/s41598-022-18452-w.